



Thermoplastic large-scale 3D printing of a light-distribution and fabrication-informed facade panel

Conference Paper**Author(s):**

Cheibas, Ina; Lloret-Fritschi, Ena; [Piccioni, Valeria](#) ; Leschok, Matthias; [Dillenburger, Benjamin](#) ; Schlüter, Arno; Gramazio, Fabio; Kohler, Matthias

Publication date:

2023-10

Permanent link:

<https://doi.org/10.3929/ethz-b-000639445>

Rights / license:

[In Copyright - Non-Commercial Use Permitted](#)

Funding acknowledgement:

-- - NCCR Digital Fabrication (SNF)

Thermoplastic large-scale 3D printing of a light-distribution and fabrication-informed facade panel

Ina Cheibas, Ena Lloret-Fritschi, Valeria Piccioni, Matthias Leschok, Benjamin Dillenburger, Arno Schlüter, Fabio Gramazio, Matthias Kohler

Department of Architecture, ETH Zürich

Zürich, Switzerland, cheibas@arch.ethz.ch

Abstract

This study analyses the thermoplastic 3D printing feasibility of a performative large-scale facade prototype. The large-scale facade panel is a geometry informed by fabrication and environmental parameters integrated gradually in the computational design process. The computational design identifies initially the 3D printing free-form potential employed by architects and designers. Then, light distribution, an environmental performance, is integrated in the computational design, by testing daylight simulations. Next, the fabrication parameters are integrated in the computational design for achieving geometry accuracy and preventing deformations. These parameters are surface angle degree, robotic speed, material extrusion values, adhesion to print bed, and inner-layer adhesion. Four iterations of the facade prototype were manufactured from polyethylene terephthalate with large-scale robotic material extrusion. The final fabrication experiment, measuring 2000 mm x 100 mm x 2000 mm, brings conclusive remarks on the key findings of this study and design guidelines for 3D printing performative facades.

Keywords

3D Printing, Additive manufacturing, Facade, Light distribution, Iterative design

1. Introduction

Additive manufactured (AM) or 3D printed facades have gained an increased interest in the construction industry. AM brings new opportunities for building sustainable and highly performative facade designs [1,2]. Through free-form design, 3D printing enables the fabrication potential of customizable performances to location, orientation, and scale [3]. However, the use of additive manufacturing for building envelopes is a recent development, and there are not yet comprehensive guidelines of this novel technique [4].

To this date, academia and industry focused mainly on displaying the free-form potential of 3D printed facades. Several materials have been proven suitable for such endeavours: thermoplastic, concrete, metal, and clay [5–8]. Thermoplastic is considered more advantageous for facade application due to material durability, lightweight, weather resistance, transparency, light transmission, and sustainability (they can be easily recyclable) [9–12]. Additionally, key performances have been already analysed for thermoplastic facades, such as thermal, air permeability, watertightness, structural loads, and fire resistance [13–15]. Other essential performances, such as light distribution have been investigated with smart materials in small-scale components [16,17].

Nevertheless, these performances are still in development and not yet suitable for architectural application. For example, the RMIT School of design project developed a 3D printed facade wall. This wall is a large-scale thermoplastic panel, which passed indoor fire and building regulations in Australia [18]. However, the application is not yet for outdoor use. Another topic is the connections between facade panels, which has just been recently developed and still need to be tested for large scale applications [14]. Additionally, Mungenast has proved the potential for large-scale self-shading geometries. Yet, the geometry performative aspect was not integrated in the design process but rather, tested at a later stage after fabrication [15]. To this date, an experimental analysis between the simulated and fabricated samples has yet to be demonstrated at an architectural scale.

Therefore, this study aims to manufacture a large-scale facade panel informed by light distribution and fabrication parameters integrated in the computational design process. Several aspects need to be considered to establish comprehensive guidelines for 3D-printed such a facade. These include: material selection, structural integrity (ensuring the structural stability and load-bearing capacity), building codes and regulations, and quality control. While it is key to establishing protocols for quality control, testing, and certification of 3D-printed building envelopes, it is critical to ensuring their performance and long-term durability. Nevertheless, we are still only at the early start in understanding the potential of this novel process. For this reason, this study focuses on analysing how the light transmission parameter can be integrated in a large-scale 3D printing panel and what are the fabrication criteria for securing a performative facade.

2. Methodology

This section presents the experimental process for an architectural-scale 3D printed facade. It displays a methodology based on an iterative workflow, which aims on generating a geometry informed by fabrication and environmental performances, see *Figure 1*. To generate such a facade geometry three main input parameters are considered: (A) computational design, (B) environmental parameters, and (C) fabrication parameters. The computational design (A) starts by identifying the facade boundary in terms of location, cardinal orientation, and dimensions. It facilitates an aesthetic expression customizable to the designer's preferences. Further, it includes the environmental parameters (B) which are integrated into the geometry design by leveraging the Ladybug and Honeybee simulation tool for light distribution. These parameters (B) are iteratively improved based on the performative evaluation of the light distribution analysis. They allow designers to consider daylight conditions and optimize their designs accordingly. Finally, fabrication parameters (C) are integrated in the geometry design regarding geometry accuracy and printability. These parameters are iteratively adapted from the performative evaluation of the fabrication analysis. The simulations contribute to visually appealing and functional objects tailored to specific environmental requirements or aesthetics.

After the geometry is generated, the iteration with the most performative result is sliced into a ready-for-fabrication toolpath (D). This toolpath is used for the 3D printing of the prototype. In the fabrication step, the 3D printed geometry is analysed for inaccuracies to adjust the fabrication parameters. If the geometry is accurate, then, the design is finalized. This workflow was tested in four fabricated experiments.

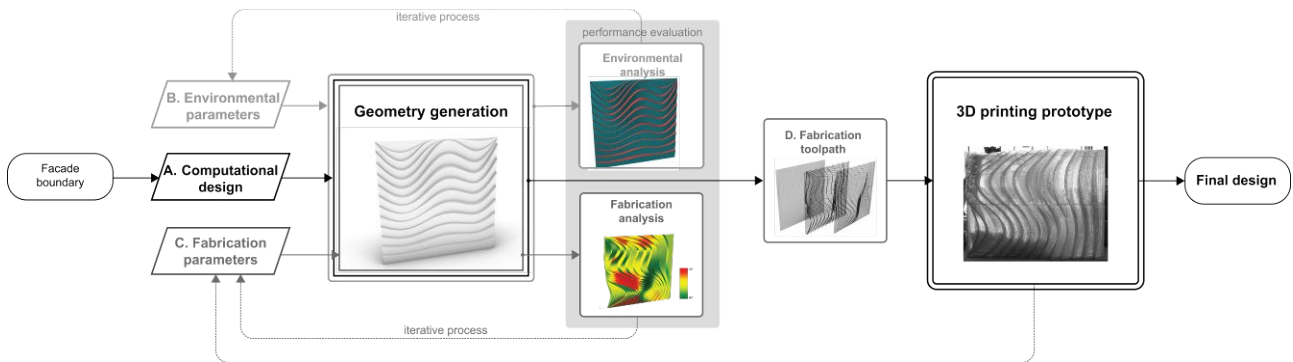


Figure 1. The workflow elements and information flows of the experimental process.

2.1 Geometry generation

The facade geometry is generated through a computational iterative process. The main factors that can contribute to performative results are computational design, environmental parameters and analysis, and fabrication parameters and analysis. These elements are integrated gradually in an iterative process, until the geometry with an optimized result is prepared for the fabrication toolpath.

A. Computational design

The computational design contributes to creating the most suitable geometry for the fabrication experiments, exemplified in the Results and Discussion section. This process is informed by two agents: boundary conditions and architectural expression. Firstly, the boundary conditions are explicit parameters for designing the 3D printed facade concerning location, cardinal orientation, and dimensions. The location of the facade is the city of Zürich, Switzerland, with south cardinal orientation. Then, a single panel is extracted to be analysed from a broader AM facade design, see *Figure 2a*. The boundary dimensions of the panel are 2 m x 0.1 m x 2 m.

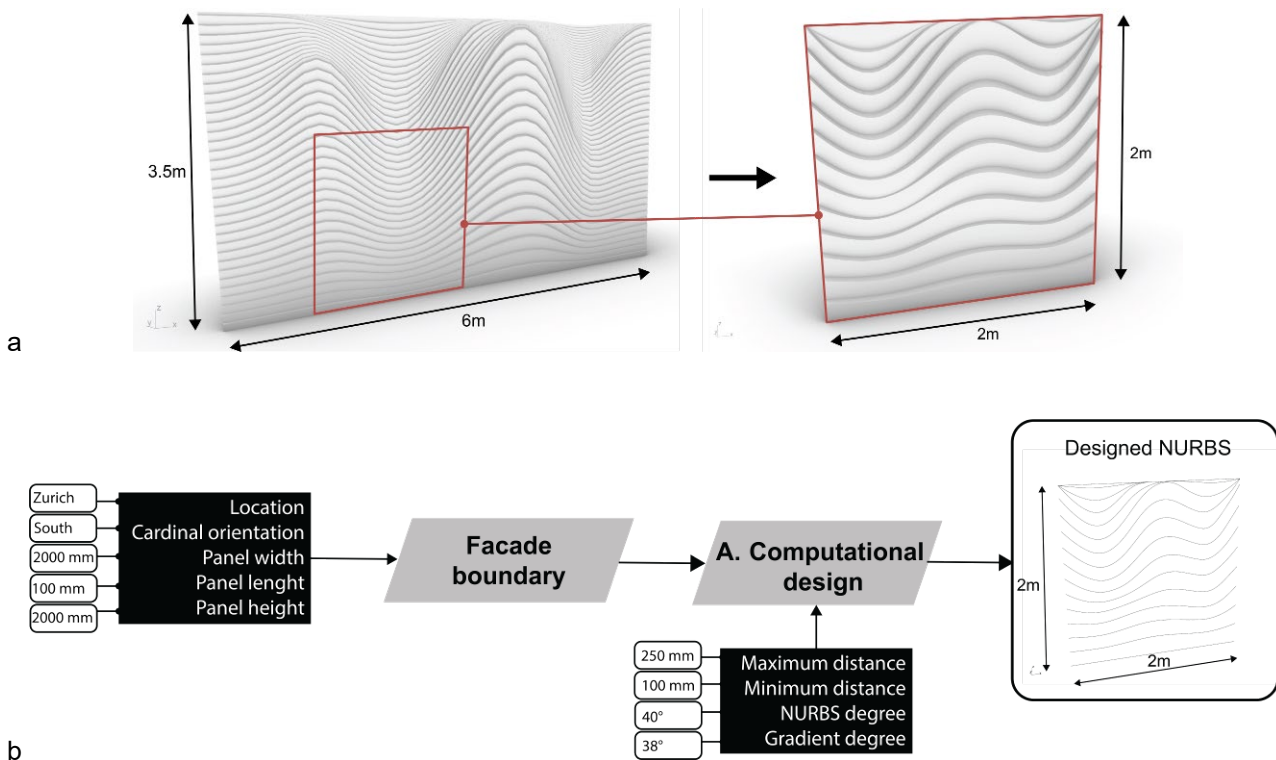


Figure 2. a) Additive manufactured facade design and the selection of one panel with 2 x 2 m dimensions; b) Computational design of the NURBS informed by facade boundary parameters, maximum and minimum distance, curvature rotation angle, and curvature gradient from bottom to top.

Integrating design parameters derived from architectural expression and context is essential in computational design—the context includes social, historical, and cultural factors. The designer can identify and select suitable parameters that align with the desired architectural expression. In this specific study, the context focuses on proving the feasibility of multi-performative integration. This implies that the design parameters chosen for the facade are aimed at achieving multiple objectives or performances, such as incorporating sustainable features, optimizing energy efficiency, enhancing aesthetics, or addressing specific functional requirements. Integrating these design parameters into the computational design process aims to create a facade that meets the boundary conditions, fulfils the desired architectural expression, and performs optimally in multiple aspects.

To achieve the desired aesthetic feature, non-uniform rational basis splines (NURBS) are utilized [19]. These NURBS are created with specific parameters that integrate the facade boundary and contribute to its overall design using; a maximum and minimum distance between the curves, a rotation angle for the NURBS curvature, and a curvature gradient from the bottom to the top of the facade, as depicted in *Figure 2b*. To facilitate the generation of these NURBS, the computational tool employed is Grasshopper, a plug-in for Rhinoceros [20]. By using NURBS and the computational capabilities of Grasshopper, the designer can achieve the desired aesthetic features while taking into account the specified parameters that integrate the facade boundary and create a visually appealing design.

B. Environmental parameters and analysis

The NURBS are used for building surfaces with volumetric modelling. These surfaces have integrated light distribution, where a specific area provides shading for summer (red colour), while other secures light transmission in winter (blue colour) *Figure 3*. The surface tilt angles are environmental parameters integrated in the geometry generation of 50° for α and 10° for β [21]. Then, environmental analysis use simulation such as LadyBug and Honeybee -Grasshopper plug-in tools- to identify if the Radiance values are performative [22].

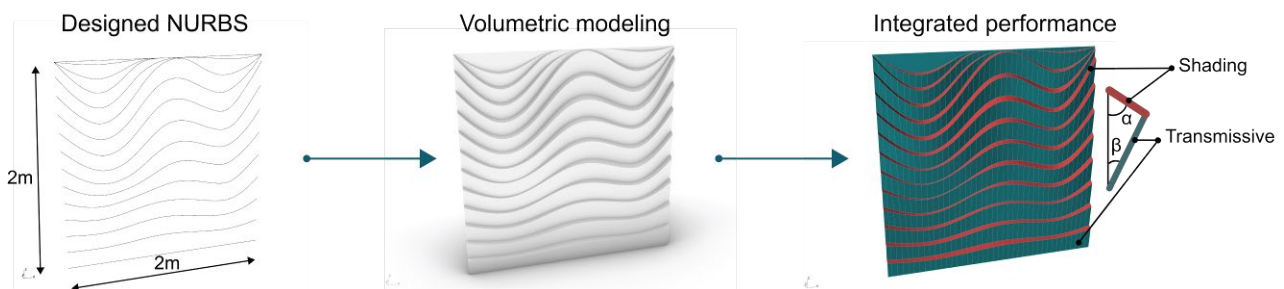


Figure 3. Geometry generation where NURBS are built into surfaces with volumetric modelling, and modified with environmental analysis for integrated performance.

C. Fabrication parameters and analysis

Besides the architectural and aesthetic considerations, fabrication parameters are also includes as these affect facade panel surface geometry. Geometry accuracy and printability must be considered to ensure panel fabrication.

Figure 4a shows the facade panel rotated 90° in the XZ world coordinates plane to improve printability and reduce geometry deformations. This rotation aligns the panel for more secure planar printing, improving print quality and reducing distortions. The panel's front and back have a multipurpose infill structure and rotate. It prevents geometry deformations, preserving panel integrity [23]. Lower thermal conductivity improves energy efficiency. Further, the infill structure matches the front panel surface for design consistency. These fabrication parameters optimise panel surface geometry for printability, structural integrity, and thermal performance, creating a successful and visually consistent 3D-printed facade.

Several fabrication parameters are considered to ensure geometry accuracy and printability. These parameters include:

- **Surface angle degree:** A surface angle degree higher than 45° is chosen to prevent overhangs and maintain stability during the printing process. *Figure 4b* displays a fabrication analysis of the surface overhang. This analysis identifies which design is suitable for fabrication depending on the angle. For

example, the left picture design has a suitable printability compared to the overhang angles in the right picture. This analysis prevents potential fabrication failures.

- **Print path width and length:** The print path width and length, specifically in the XY plane, are determined based on the desired level of detail and the capabilities of the 3D printing equipment. The 2 mm layer height and 5 mm layer width was selected to ensure accurate geometries and proper layer adhesion.
- **Adhesion to the print bed:** Ensuring good adhesion between the printed object and the print bed is crucial for preventing warping, lifting, or shifting during the printing process. Various techniques, such as using adhesion aids or adjusting print bed temperature, can be employed to enhance adhesion. For the following experiments mechanical connection in form of an integrated brim were selected, described in more detail in the 2.2.1 *Material* subsection.
- **Inner-layer adhesion:** Inner-layer adhesion refers to the bonding between consecutive layers in the printed object. This parameter is important for maintaining structural integrity and preventing delamination. Proper extrusion settings, material selection, and printing parameters can help ensure strong inner-layer adhesion.

By considering these fabrication parameters, the design process can be guided towards achieving the desired results, ensuring accurate and high-quality 3D-printed geometries for the facade.

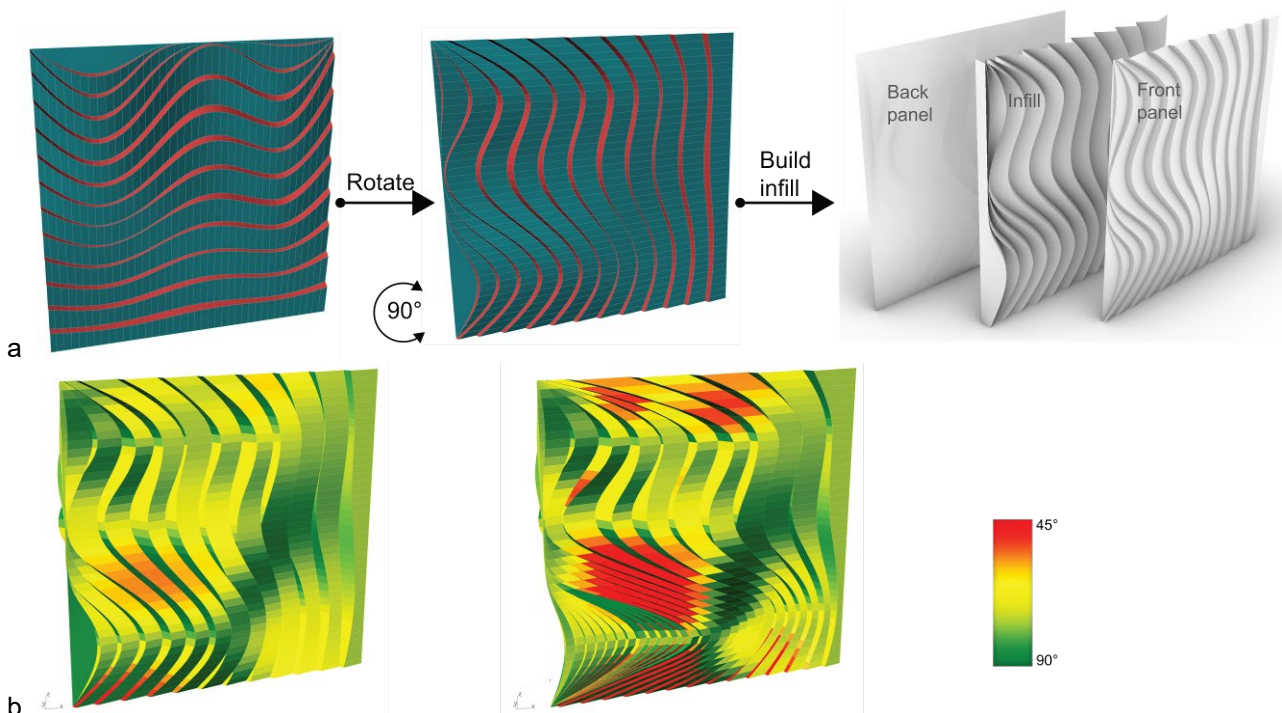


Figure 4. a) Geometry modified for better printability and lower deformations by rotating it and building an infill in the panel; b) Left picture represents a geometry iteration with better printability, while the right picture has a higher degree of surfaces under 45° angle which will fail during fabrication.

D. Fabrication toolpath

The final step in the geometry generation is the slicing into a ready-for-fabrication toolpath, see *Figure 5a*. The 3D print toolpaths are contours built from planar curves vertically slicing the surface in a customized Python module. The slicing process is informed by all parameters of the geometry generation. The fabrication parameters - robot speed and material extrusion values - influence the toolpath printing direction. For example, to keep a continuous material extrusion, the panel have to have a specific printing direction. Otherwise, an intersection will occur between print lines, which generates geometry inaccuracies. Thus, each second layer of the toolpath has a reversed printing direction, which secures a continuous fabrication loop and accurate geometry (*Figure 5b*).

The environmental parameter influences the geometry design for transmissive and shading area in the front surface (Figure 5c). The transmissive area has a straight print path, while the shading area has a zigzag pattern with 6 mm distance between points (Figure 5d). This zigzag pattern is reversed for every 2nd layer to create a pattern resembling droplets [24]. Then, the final digital toolpath is exported into a JavaScript Object Notation (JSON) file used through COMPAS_RRC, an online control for ABB robots in a Python interface [25,26].

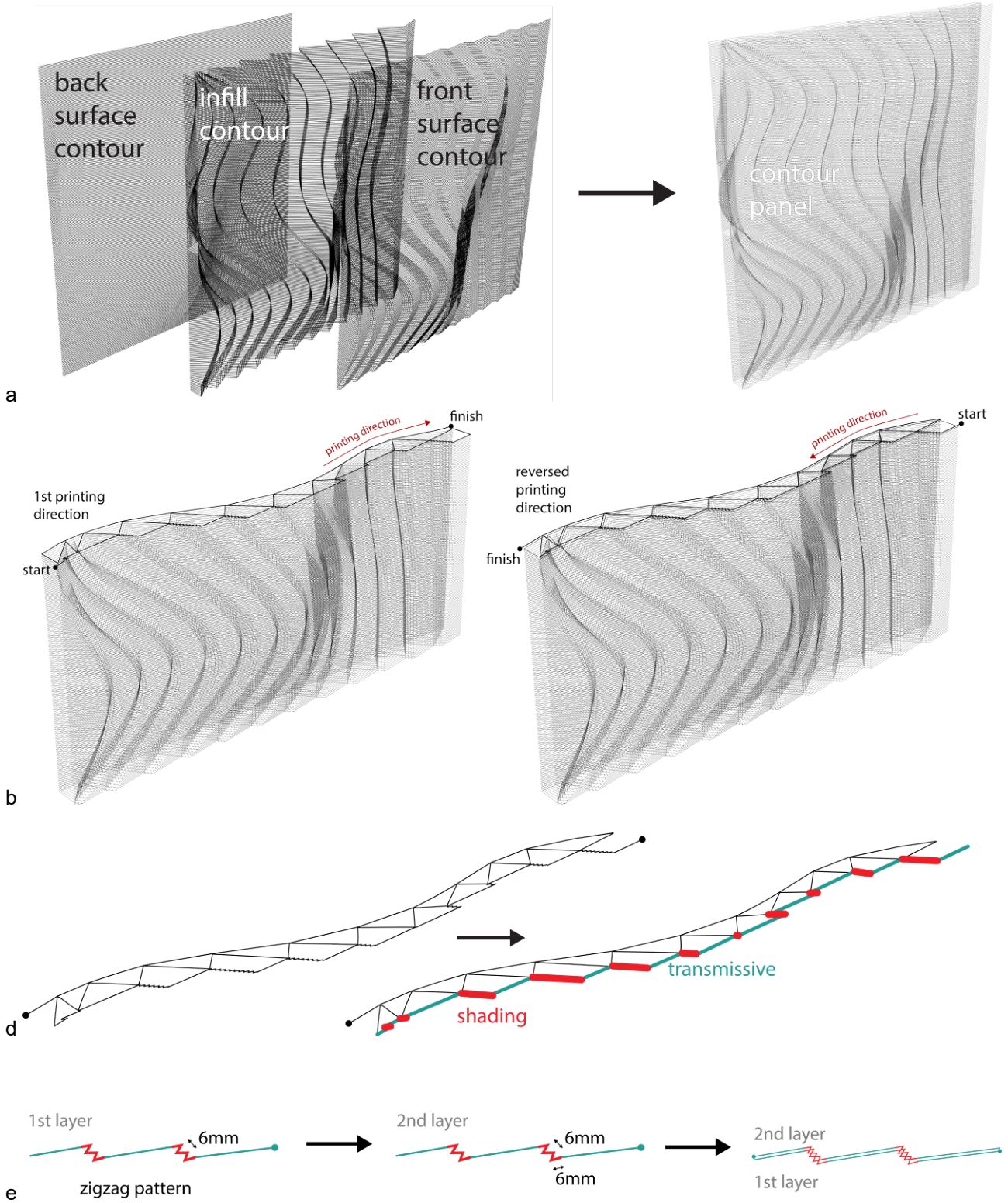


Figure 5. a) Slicing of the BREP surface into contour curves, which forms the layers of the geometry; b) Aligned printing direction and reversed printing direction in every second layer; c) Shading and transmissive designated area on the front surface contour; d) Shading toolpath in zigzag pattern and transmissive surface area with linear path, where every second layer has a reversed pattern direction.

2.2 3D printing prototype

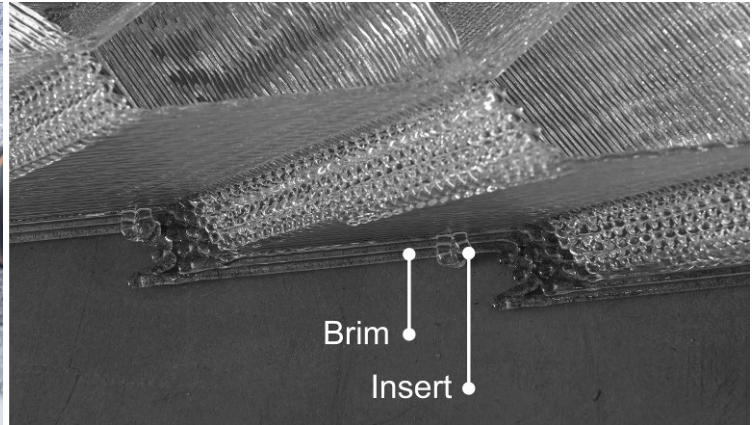
2.2.1 Material

The material play a key role in 3D printing the facade prototype. In this study, polyethylene terephthalate glycol (PETG) has been selected as a suitable fabrication material due to its low warping tendency and easier-to-recycle properties (Figure 6a) [27]. PETG has excellent inner layer adhesion, which can prevent delamination and secure geometry build up in the case of 3D printing errors (Figure 6c). However, PETG has very poor adhesion to print bed, which can lead to high environmental stress cracking resistance and post-extrusion warpage in the prototype. For this reason, a brim with screw inserts has been added at the geometry base, to secure adhesion to the wooden print bed Figure 6b.

Although, PETG has great potential for large-scale fabrication, this material does not yet comply with building codes and regulations due to low fireproof resistance. However, due to its excellent optical properties, low water absorption, and good structural strength, PETG was selected in this study as the most suitable 3D printing material for facade application based on the market availability.



a



b



c



Figure 6. a) Polyethylene terephthalate glycol (PETG) in pellet form; b) Brim and inserts for metal screws to secure adhesion to print bed and prevent geometry deformation; c) Toolpath failure due to small width of the 3D print line (lower than 2 mm) and geometry failure due to low overhang angle (lower than 45°).

2.2.2 Fabrication setup

A large-scale fabrication setup is located in the Robotic Fabrication Laboratory (RFL) at ETH Zürich [28]. In this laboratory, an ABB 4600 Robotic Arm is attached to a gantry and it has six-axis motion possibilities, Figure 7 [29]. The main fabrication tools are a CEAD thermoplastic extruder, and a wooden print bed with dimensions of 2500 x 2500 mm [30]. The CEAD pellet extruder has an output of 12 kg/h, and can work at various robotic speeds up to 250 mm/s. It contains four heating zones with customizable temperature control. The PETG was dried for 4 hours at 60° Celsius with a VisMec Dryplus 50 equipped with a hopper loader to prevent air and humidity vapours from getting trapped in the material [31].



Figure 7. ABB 4600 Robotic Arm attached to a gantry (left picture) and CEAD thermoplastic extruder (right picture).

3. Experimental results

This section displays the four fabrication experiments of the facade panel. These experiments were iterations of the same geometry evaluated and optimized for accuracy to understand the deviation between the designed and the build prototype. Each iteration was analysed for the following criteria:

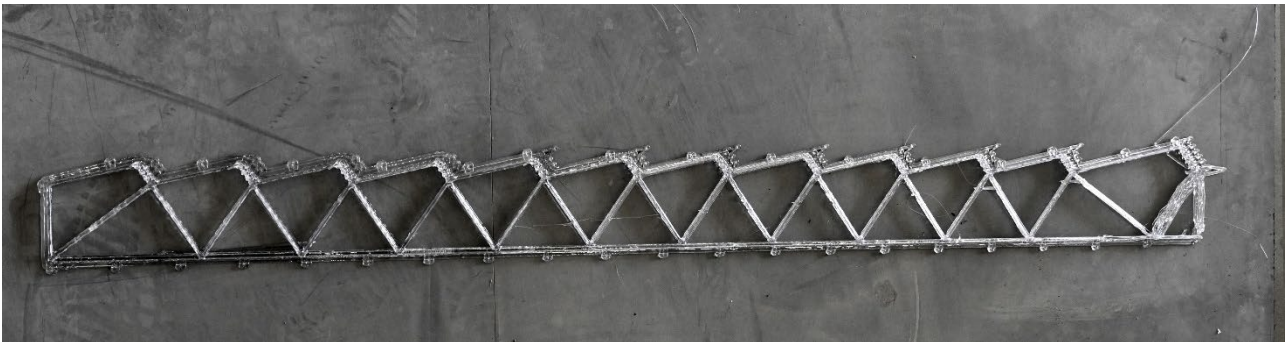
- **Geometry warping.** The overall fabricated shape is considered adequate if it has similar dimensions to the simulated model without any visible deformations to the naked eye.
- **Overhang.** The fabricated shape has no 3D print toolpath failure, where the material extends outwards it's designed shape due to low printing angle. The zigzag pattern accuracy relies on evading overhang.
- **Adhesion to print bed.** The position of the prototype remains stable on the print bed during and after fabrication.
- **Delamination.** Inner layer adhesion is steady without any layer delamination.
- **Cracks.** There are no cracks occurring in the prototype due to high post-tension warping.

3.2 Iteration 1

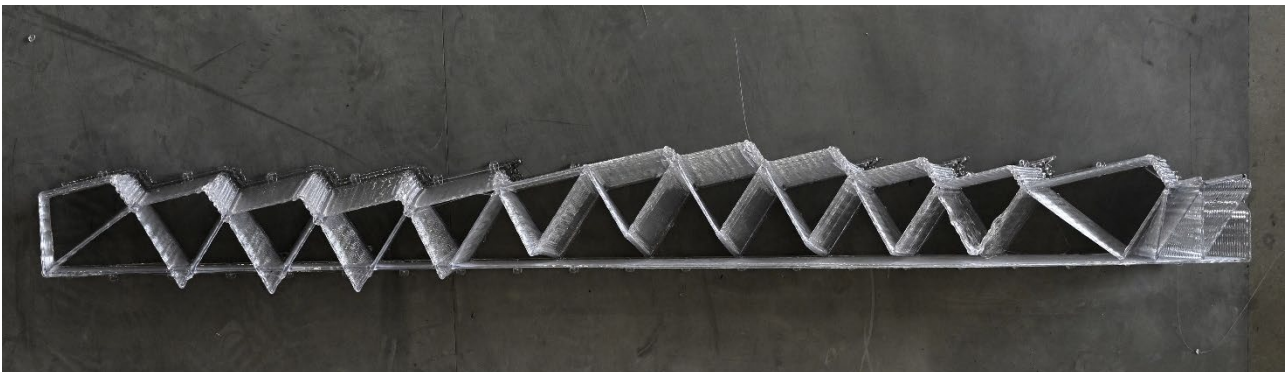
The goal of Iteration 1 was to identify if adhesion to print bed, reversed printing direction for every 2nd layer, and maximum fabrication space is secure. The first and second experiments used the same computational design, see *Figure 2a*. In this iteration, the maximum reach of the robot arm was adjusted for avoiding singularity. The robot joints were moved until an adequate Cartesian angle position is secure in the fabrication process. The gantry was set-up to rise 2 mm automatically after every printed layer. The automatic rise would occur only after printing 800 mm height of the sample so that maximum reach of the robot arm can achieve 2000 mm height. It was found that during prototype fabrication the insert screws are properly distanced, adhesion to the print bed is secure, every second layer has a reversed print direction, and layer width is accurate based on the extrusion vales, *Figure 8a*.

3.3 Iteration 2

The aim of Iteration 2 was to identify if overhang occurs in the prototype fabricated in the first iteration. For this reason, the Iteration 2 prototype was 3D printed until 120 mm height. The first iteration fabrication parameters were considered suitable and used for the second iteration (*Figure 8b*). Then, fabrication time, panel weight, pattern accuracy, and infill overhang were analysed and documented. Fabrication time was essential to estimate on the required timeline to build the entire height of the panel, while panel weight was key for determining the required material for this process. The fabricated prototype proved accurate pattern results (*Figure 8c*). However, the infill failed in specific areas with a lower than 45° overhang angle (*Figure 8d*). Consequently, the computational design was modified from 45° to a 50° angle for the next iteration.



a



b

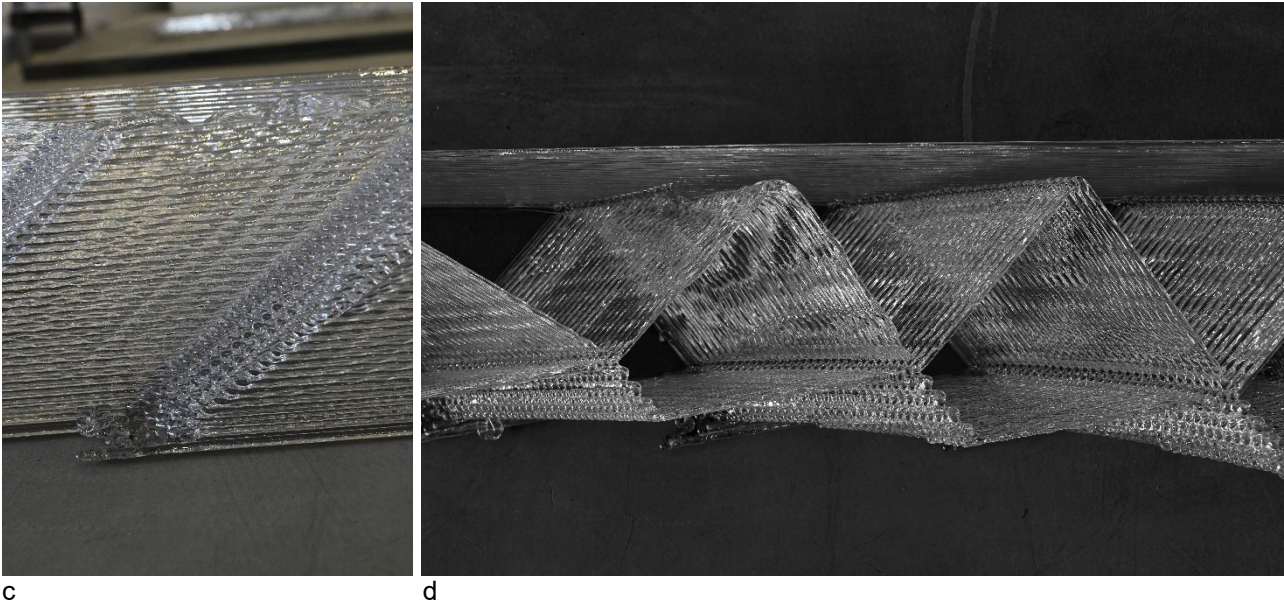


Figure 8. a) First experiment with 30 mm height; b) Second experiment with 120 mm height; c) Suitable zigzag pattern accuracy; d) Infill geometry failure due to high overhang.

3.4 Iteration 3

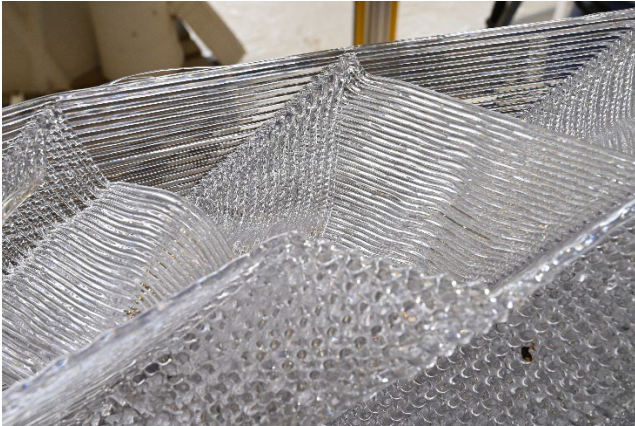
The goal of the third iteration was to determine if geometry warping, delamination, and crack occurs in the fabricated prototype. Based on the second iteration, the infill was modified from 45° to a 50° angle to prevent overhang. Robot speed, extrusion values, and print path width were analysed in this process. The fabricated prototype was 3D printed until 1550 mm height (*Figure 9a*). The robot speed was incrementally increased to 100 mm/s, and then lowered to 90 mm/s because increased robotic speed contributed to overhang (*Figure 9b*).

The fabrication process of the prototype was stopped at 778 mm height, due to collision between the robotic arm and the facade panel. A re-start of the print was possible with the gantry moved in a higher position to avoid further collisions. Yet, the resume resulted in a visible inaccuracies in the prototype, due to geometry warping (*Figure 9c*). The warping is estimated to be caused by high stresses during material curing, which occurred in the time between the collision and re-start.

Nevertheless, the final fabrication settings contributed to good pattern accuracy, as overhang did not occur in the zigzag pattern (*Figure 9d*). Additionally, no delamination or cracks were visible in the overall prototype, which contributed to a good print layer quality (*Figure 9e*.)



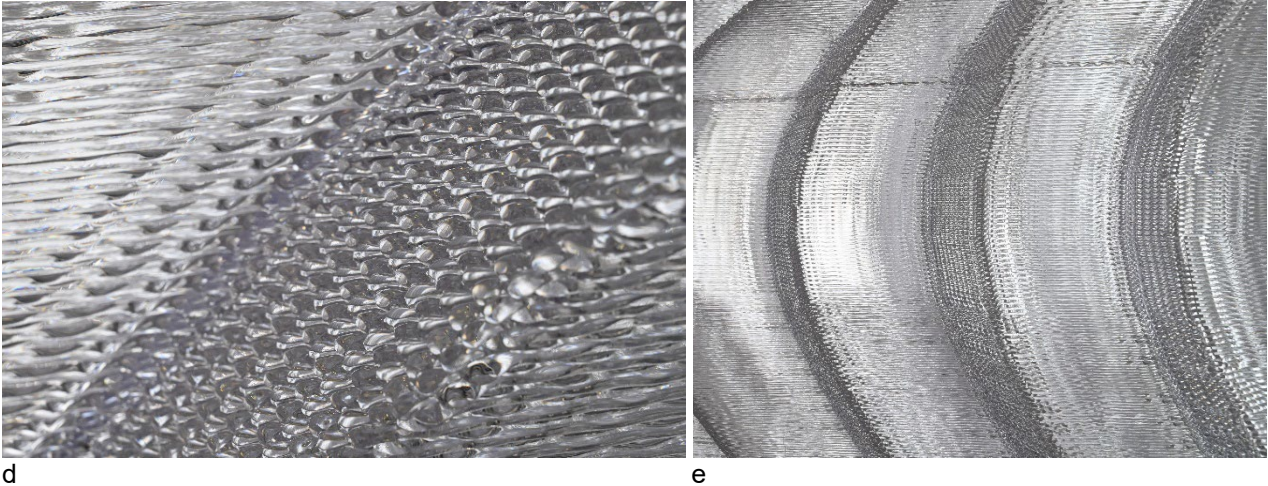
a



b



c



d

e

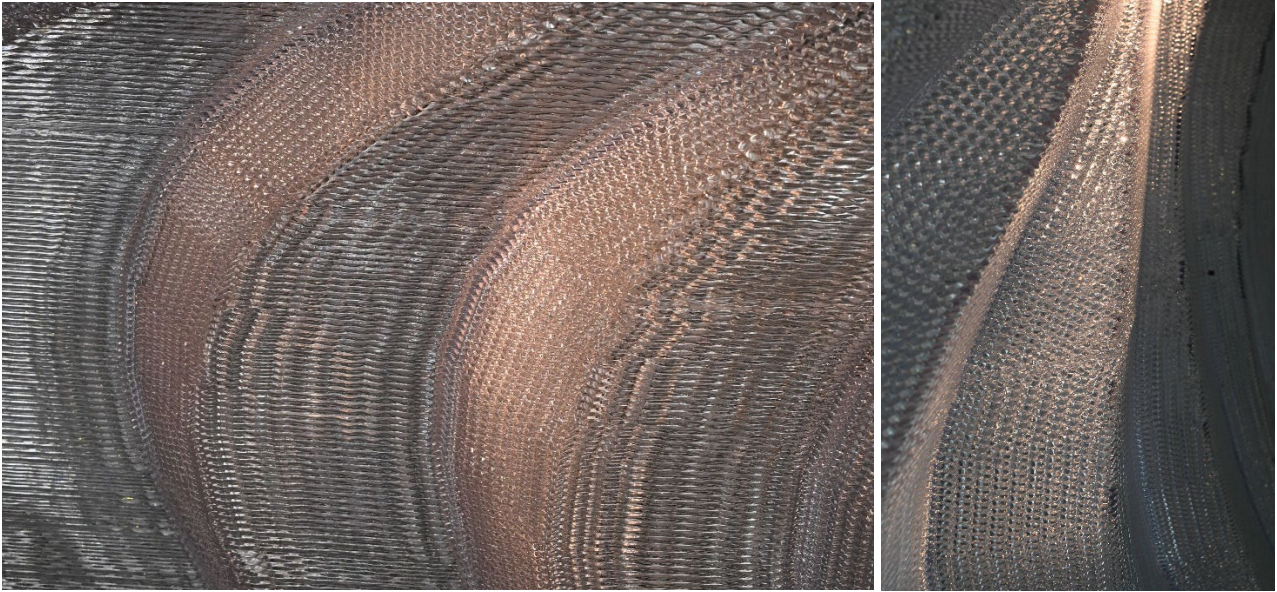
Figure 9. a) Third experiment with height of 1550 mm; b) Geometry failure due to high speed and lower extrusion; c) Failure in the geometry at the re-start seam; d) Good print quality of the micro pattern; e) Overall good print quality in the panel without cracks or delamination.

3.5 Iteration 4

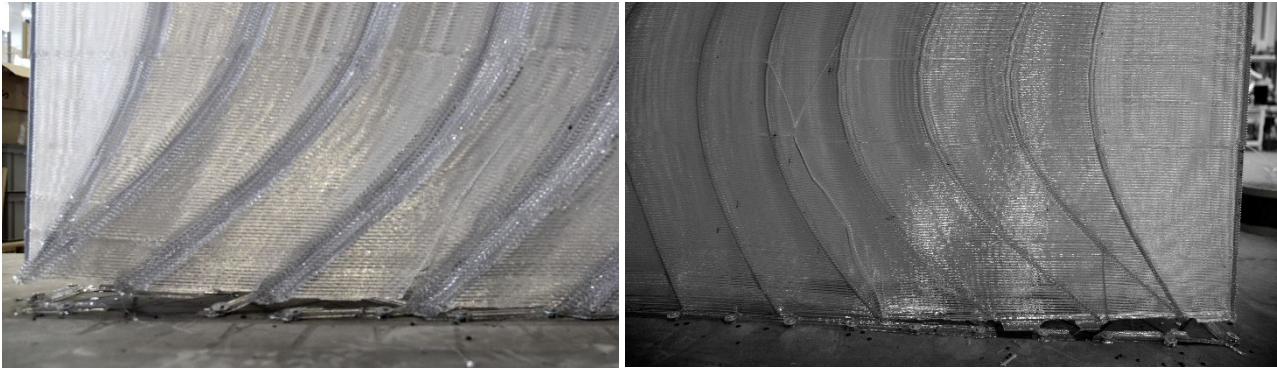
The final iteration combined all the learnings from previous prototypes and successfully printed a 2 x 2 m panel. The objective was to achieve maximum height and geometry precision, which was possible by reducing the curvature of the angles in the computational design. The final prototype had a more tamed curvature which decreased the overhang potential failure. This was possible by decreasing infill distance from 250 mm to 200 mm, which also contributes to preventing cracks in the sample. Additionally, several fabrication parameters were increased to further reduce fabrication time, such as higher printing speed to 140 mm/s, high extruder temperatures, and high extrusion value to 35 RPM. *Table 1* displays the fabrication settings used in all four iterations. Furthermore, the print path was also modified in the micro pattern density, with a distance from 5 mm to 6 mm to decrease fabrication time. The distance did not alter the print quality, as the pattern had a good form definition and inner-layer adhesion (*Figure 10a*).

Although the infill prevented the overall geometry deformations, the prototype still had significant cracks at the corners, see *Figure 7b*. These crack and inadequate print bed adhesion occurred at different intervals in time, more visible after 900 mm height printing, which displaced the geometry during fabrication. This displacement contributed to visible seams in the geometry *Figure 10c*.

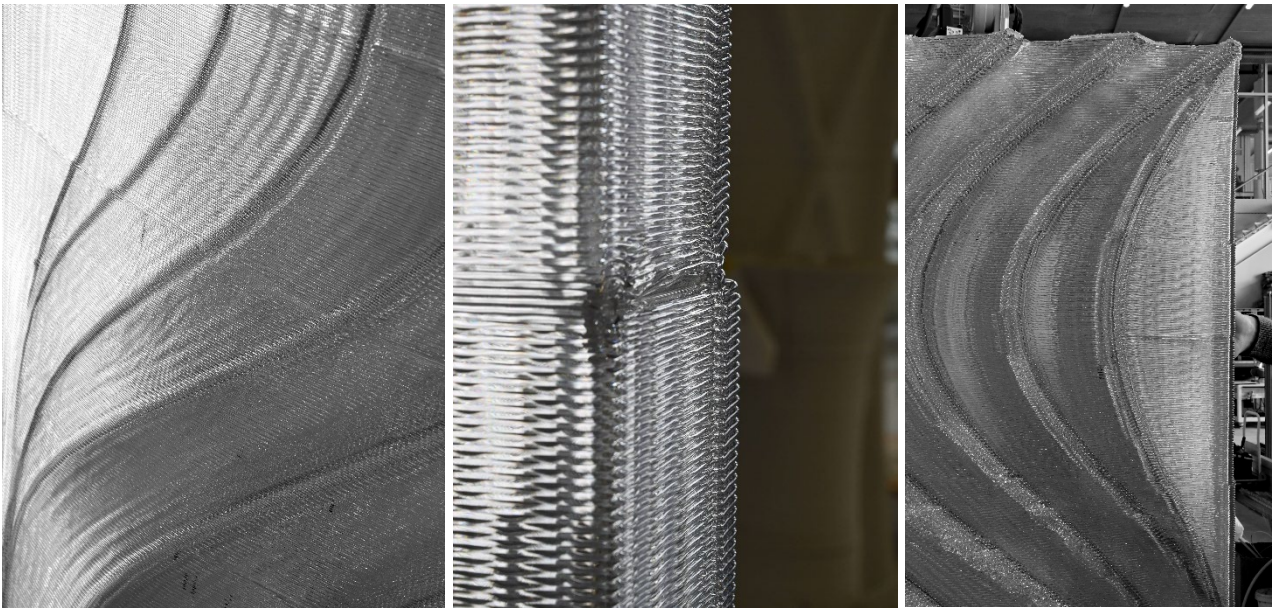
Nevertheless, these final parameters in Iteration 4, contributed to a successful 3D printed facade panel, see *Figure 11a*. The overall geometry has an accurate geometry, and was considered suitable for the next step of experiments. A wooden frame was placed on the sample edges. Then, the panel was installed in the Zero Carbon Building Systems Lab to prepare it for further testing of light distribution and heat gains, see *Figure 11b-c*.



a



b



c

Figure 10. a) Good quality of the micro-pattern; b) Crack occurred at both corners of the prototype due to high stresses in the fabricated prototype; c) Seams created by the deformation and cracks of the panel during fabrication.



a



b



c

Figure 11. a) Fabrication of the fourth iteration with height of 1998 mm; b) Back view of the 3D-printed facade panel; c) Front view of the panel.

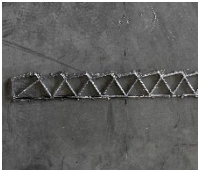

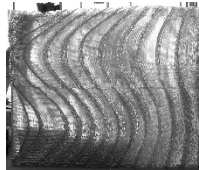
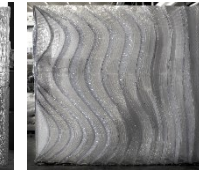
Prototypes		Iteration 1	Iteration 2	Iteration 3	Iteration 4
					
1	Material	PETG	PETG	PETG	PETG
2	Environment temperature	11 ° C	11 ° C	17 ° C	12 ° C
3	Average print path length/layer	9.05 m	9.05 m	9.05 m	8.83 m
4	Layer height	2 mm	2 mm	2 mm	2 mm
5	Layer width	4.4 ± 1 mm	4.8 ± 1 mm	4.7 ± 1 mm	4.8 ± 1 mm
6	Overhang angle	45°	45°	50°	50°
7	Nozzle diameter	4 mm	4 mm	4 mm	4 mm
8	Extruder 4 temperatures	225, 245, 255,	225, 245, 255,	235, 255, 265,	235, 255,
9	(T1, T2, T3, Nozzle T4)	265°C	265°C	265°C	265, 265°C
10	Robot speed	70 mm/s	70 mm/s	90 mm/s	140 mm/s
11	Extrusion values	16.8 RPM*	16.8 RPM*	21.7 RPM*	35 RPM*
12	Sample height	30 mm	120 mm	1550 mm	1998 mm
13	Cooling	no	no	no	no
14	Weight	1.06 kg	5.52 kg	71.36 kg	92.5 kg
15	Fabrication time	36 min	2h 35min	26h 7min	23h 43min

Table 1. Fabrication settings of the additive manufactured prototypes. *RPM = rotation per minute

4. Discussion and Conclusion

This study 3D printed a large-scale performative thermoplastic facade panel. The experimental tests proved that an integration of environmental and fabrication parameters is possible in the initial computational design process. What is essential in this process is an iterative integration of all the parameters for securing an accurate geometry fabrication. The iterative process is essential for refining and improving the simulated prototype based on the experimental results. The design tool can therefore, adapt and mitigate further fabrication risks in the overall prototype, such as geometry warping, overhang, poor adhesion to print bed, delamination and cracks occur in the sample. These failures can be only visible by an experimental process. Thus, the computational design tool has to consider not only the parameters that contribute to a performative geometry, but also the parameters derived from experimental results. This study proved that manufacturing errors could be rectified at the design stage, which decreases the need for a multitude of experimental testing and material waste. The key findings of the study are:

1. Continuous fabrication is more suitable for a seamless result. A 3D printing restart is not recommended for the material used in this study.
2. Multiple geometry iterations in the design stage are key for achieving an accurate outcome. For example, smaller infill distances, overhang angle, and wider print path required tuning after several fabrication experiments.
3. New or improved 3D printing materials are essential for good fabrication results, to avoid cracking and geometry warping.

Therefore, based on these key findings, the essential guidelines recommended for designing a performative 3D printed facade are:

- **Material selection.** The material is key for providing feasible results in the architectural and building field. A combination between a highly suitable 3D printing material, while also being compliant to the building codes and regulations is essential for facade application. Furthermore, an ideal candidate would also be recyclable, considering the sustainability concerns.
- **Environmental parameters.** Integrating environmental performances in the computational design process contributes to improved energy efficiency, enhanced occupant comfort, sustainability, and cost optimization. These advantages are pertinent for building highly performative 3D printed facades. Multiple parameters can be assimilated into a facade panel, such as daylight distribution, thermal, air permeability, watertightness, and structural loads. However, it is fundamental to iteratively integrate

these parameters for avoiding discrepancies between them. Additionally, the computational design must also accommodate fabrication parameters next to the environmental ones.

- **Fabrication parameters.** Fabrication parameters are essential for securing good quality prints and high-performative geometries. Surface angle degree, robotic speed, extrusion values, print path width and length, and adhesion to print bed are fabrication parameters highly relevant to prevent geometry warping, overhang, delamination, cracks and poor adhesion to print bed.
- **Experimental testing.** Experimental testing for both fabrication and environmental performance can validate all these parameters. Experimental work enables quality control, testing, and certification of the simulated versus the tested results. In this step, is especially imperative to use an iterative process for fabricating complex 3D printed geometries.

Therefore, in a further study the final iteration of the facade panel will be tested for light distribution in the Zero Carbon Building Systems Lab.

This study highlights the versatility of additive manufacturing technology for facade customization, sustainability, and performance optimization. It enables architects and designers to create unique facades with embedded daylighting capabilities, tailored to specific performative criteria.

Acknowledgments

The authors would like to express gratitude to Erika Marthins, Philippe Fleischmann, Michael Lyrenmann, and Tobias Hartmann for their support in this project.

Funding statement

This work was supported by the Swiss National Science Foundation (SNF), within the National Centre of Competence in Research Digital Fabrication (NCCR DFAB Agreement No. 51NF40-141853).

5. References

- [1] R. Naboni, N. Jakica, Additive manufacturing in skin systems: trends and future perspectives, *Rethink. Build. Ski. Transform. Technol. Res. Trajectories*. (2021) 425–451. <https://doi.org/10.1016/B978-0-12-822477-9.00004-8>.
- [2] I. Agustí-Juan, G. Habert, Environmental design guidelines for digital fabrication, *J. Clean. Prod.* 142 (2017) 2780–2791. <https://doi.org/10.1016/j.jclepro.2016.10.190>.
- [3] W. Tuvayanond, L. Prasittisopin, Design for Manufacture and Assembly of Digital Fabrication and Additive Manufacturing in Construction : A Review, (2023) 1–25. <https://doi.org/10.20944/preprints202211.0290.v2>.
- [4] M. Leschok, I. Cheibas, V. Piccioni, B. Seshadri, A. Schlüter, F. Gramazio, M. Kohler, B. Dillenburger, 3D printing facades: Design, fabrication, and assessment methods, *Autom. Constr.* 152 (2023) 104918. <https://doi.org/10.1016/j.autcon.2023.104918>.
- [5] M. Ghasemieshkaftaki, M.A. Ortiz, P.M. Bluysen, An overview of transparent and translucent 3D-printed façade prototypes and technologies, in: *Proc. Heal. Build. Eur. 2021 Online Conf. Oslo, Norw.*, 2021: pp. 21–23.
- [6] A. Jipa, B. Dillenburger, 3D Printed Formwork for Concrete: State-of-the-Art, Opportunities, Challenges, and Applications, *3D Print. Addit. Manuf.* 9 (2022) 84–107. <https://doi.org/10.1089/3dp.2021.0024>.
- [7] C. Buchanan, L. Gardner, Metal 3D printing in construction: A review of methods, research, applications, opportunities and challenges, *Eng. Struct.* 180 (2019) 332–348. <https://doi.org/10.1016/j.engstruct.2018.11.045>.
- [8] A. Wolf, P.L. Rosendahl, U. Knaack, Additive manufacturing of clay and ceramic building components, *Autom. Constr.* 133 (2022) 103956. <https://doi.org/10.1016/j.autcon.2021.103956>.
- [9] L.O. Vaught, A.A. Polycarpou, Investigating the effect of fused deposition modelling on the tribology of PETG thermoplastic, *Wear.* 524–525 (2023) 204736. <https://doi.org/10.1016/j.wear.2023.204736>.
- [10] D. Pfarr, C. Louter, Prototyping of digitally manufactured thin glass composite façade panels, *Archit. Struct. Constr.* (2023). <https://doi.org/10.1007/s44150-022-00080-7>.
- [11] B. Seshadri, I. Cheibas, M. Leschok, V. Piccioni, I. Hischier, A. Schlüter, Parametric design of an additively manufactured building façade for bespoke response to solar radiation, *J. Phys. Conf. Ser.* 2042 (2021). <https://doi.org/10.1088/1742-6596/2042/1/012180>.
- [12] O. Ulkir, Energy-Consumption-Based Life Cycle Assessment of Additive-Manufactured Product with Different Types of Materials, *Polymers (Basel)*. 15 (2023) 1466. <https://doi.org/10.3390/polym15061466>.
- [13] M.V. Sarakinoti, M. Turrin, T. Konstantinou, M. Tenpierik, U. Knaack, Developing an integrated 3D-printed façade with complex geometries for active temperature control, *Mater. Today Commun.* 15 (2018) 275–279. <https://doi.org/10.1016/j.mtcomm.2018.02.027>.
- [14] I. Cheibas, R.P. Gamote, B. Önalán, E. Lloret-Fritsch, F. Gramazio, M. Kohler, Additive Manufactured (3D-Printed) Connections for Thermoplastic Facades, in: A. Gomes Correia, M. Azenha, P.J.S. Cruz, P. Novais, P. Pereira (Eds.), *Trends Constr. Digit. Era*, Springer International Publishing, Cham, 2023: pp. 145–166. https://doi.org/10.1007/978-3-031-20241-4_11.
- [15] M.B. Mungenast, 3D-Printed Future Facade, Technische Universität München, 2019.

- [16] D. Clifford, Aesthetics and Perception: Dynamic Facade Design with Programmable Materials, in: J. Wang, D. Shi, Y. Song (Eds.), *Adv. Mater. Smart Build. Ski. Sustain. From Nano to Macroscale*, Springer International Publishing, Cham, 2023: pp. 243–256. https://doi.org/10.1007/978-3-031-09695-2_12.
- [17] V. Piccioni, M. Leschok, L.O. Grobe, S. Wasilewski, I. Hischer, A. Schlüter, Tuning the Solar Performance of Building Facades through Polymer 3D Printing, *Adv. Mater. Technol.* (2022). <https://doi.org/10.3929/ETHZ-B-000575654>.
- [18] Studio Roland Snooks — Sensilab studio, (2017). <http://www.rolandsnooks.com/#/sensilab-studio/> (accessed October 26, 2022).
- [19] D.F. Rogers, *An introduction to NURBS: with historical perspective*, Morgan Kaufmann, 2001.
- [20] Grasshopper, Visual programming language, plugin for Rhinoceros, (2007). <https://www.rhino3d.com/6/new/grasshopper> (accessed July 20, 2023).
- [21] I. Cheibas, E. Lloret-Fritschi, V. Piccioni, E. Marthins, R. Rust, M. Leschok, A. Schlüter, B. Dillenburger, F. Gramazio, M. Kohler, Design for the solar irradiation of an additively manufactured facade, *Des. Stud.* (2023).
- [22] Honeybee | Ladybug Tools, (2012). <https://www.ladybug.tools/honeybee.html> (accessed May 17, 2023).
- [23] V. Piccioni, M.; Turrin, M. Tenpierik, A Performance-Driven Approach for the Design of Cellular Geometries with Low Thermal Conductivity for Application in 3D-Printed Façade Components, in: *Proc. Symp. Simul. Archit. Urban Des. (SimAUD 2020)*, Society for Computer Simulation International (SCS), 2020: pp. 327–344.
- [24] I. Cheibas, V. Piccioni, E. Lloret-Fritschi, M. Leschok, A. Schlüter, B. Dillenburger, F. Gramazio, M. Kohler, Additive Daylighting: Light Distribution in 3D Printed Thermoplastics, *3D Print. Addit. Manuf.* (2023). <https://doi.org/10.1089/3dp.2023.0050>.
- [25] D. Crockford, The application/json media type for javascript object notation (json), (2006). <https://www.rfc-editor.org/rfc/rfc4627.html> (accessed May 17, 2023).
- [26] P. Fleischmann, G. Casas, M. Lyrenmann, COMPAS RRC: Online control for ABB robots over a simple-to-use Python interface., (2020). <https://doi.org/10.5281/zenodo.4639418>.
- [27] Extrudr, PETG transparent, (2022). https://www.extrudr.com/en/products/catalogue/petg-transparent_1803/ (accessed May 17, 2023).
- [28] Robotic Fabrication Laboratory | Institute of Technology in Architecture, ETH Zürich, (2016). <https://ita.arch.ethz.ch/archteclab/rfl.html> (accessed April 23, 2023).
- [29] ABB, IRB 4600, (2009). <https://new.abb.com/products/robotics/robots/articulated-robots/irb-4600> (accessed May 17, 2023).
- [30] CEAD Extruder | Pellet extruder for composite thermoplastic 3D printing, (2020). <https://robotextruder.com/> (accessed July 23, 2023).
- [31] VisMec, Ddryplus 50, (2015). <https://www.vismec.com/en/drying/dryplus/> (accessed May 17, 2023).